

1 **Improved phosphometabolome profiling applying isotope dilution strategy and capillary ion**
2 **chromatography-tandem mass spectrometry**

3

4 Marit H. Stafsnes[#], Lisa M. Røst[#], and Per Bruheim^{#¶}

5 [#]NTNU Norwegian University of Science and Technology,

6 Department of Biotechnology and Food Science

7

8 Corresponding author:

9 [¶]Per Bruheim

10 Sem Sælands vei 6/8,

11 N-7491 Trondheim, Norway

12 Per.Bruheim@ntnu.no

13

14 **Key words:**

15 Phosphometabolome, capillary ion chromatography, mass spectrometry, isotope dilution

16

17 **Declarations of interest: none**

18 **Abstract**

19 The phosphometabolome is comprised of all phosphorylated metabolites including the major
20 metabolite classes sugar phosphates and nucleoside phosphates. Phosphometabolites are invaluable
21 in any cell as a part of primary- and energy- metabolism, and as building blocks in the biosynthesis of
22 macromolecules. Here, we report quantitative profiling of the phosphometabolome by applying
23 capillary ion chromatography-tandem mass spectrometry (capIC-MS/MS), ensuring improved
24 chromatographic separation, robustness and quantitative precision. Baseline separation was
25 achieved for six out of eight tested hexose phosphates. Quantitative precision and reproducibility
26 was improved by introducing a fully uniformly (U) ^{13}C -labeled biological extract and applying an
27 isotope dilution (ID) correction strategy. A ^{13}C -labeled biological extract does in principle contain
28 internal standards (IS) for all metabolites, but low abundant metabolites pose a challenge, and
29 solutions to this are discussed. The extreme reproducibility and reliability of this capIC-MS/MS
30 method was demonstrated by running the instrumentation continuously for ten days.

31

32 **Introduction**

33 Metabolites comprise less than three percent of the cell dry matter, but serve critical functions in
34 energy generation and as building blocks for macromolecules across all domains of life. Hence, the
35 analysis of the metabolome, metabolomics, is of high interest in biological studies; especially studies
36 of the phenotype. The metabolome is a heterogeneous collection of compounds with great variation
37 in both abundances and physio-chemical properties, which cause significant analytical challenges. In
38 addition, high turnover rates and chemical instability is observed for many metabolites [1, 2]. Mass
39 spectrometry (MS) and nuclear magnetic resonance (NMR) are the two most frequently used
40 technologies in the field of metabolomics, with MS dominating due to much higher sensitivity and
41 coverage of the metabolome.

42 The approaches to MS based metabolomics are many, e.g. non-target vs. target, with or
43 without chromatographic separation prior to MS detection, fingerprinting vs. profiling, with the
44 preferred approach depending on the biological model system and the pending research questions
45 [3]. Target quantitative metabolite profiling aims at quantifying known metabolites from one or
46 several metabolite groups, e.g. amino acids and other amino group containing metabolites. Usually
47 20-50 metabolites are included in such metabolite profiling methods [4-6], which sometimes include
48 a stable label derivatization for increased quantitative accuracy and precision [7].

49 For profiling of the phosphometabolome (sugar-phosphates, nucleoside phosphates and
50 other phosphorylated metabolites), there are mainly two methodological approaches: liquid
51 chromatography (LC)-MS/MS using ion pair reagents [8, 9] and ion chromatography (IC)-MS/MS. The
52 ion pair reagent improves chromatographic separation of the highly negatively charged
53 phosphometabolites on a reverse phase (RP) LC-column, but is very sticky and hard to remove from
54 capillaries and connections of the LC-MS/MS instrument. Thus, it is strongly recommended to
55 dedicate a separate LC-MS/MS systems for ion pair reagent based analysis to eliminate the risk of
56 contaminating other analyses. IC is the less frequently used alternative, but has superior separation
57 capabilities of phosphometabolites. The instrumentation is more complex, with several units such as

58 membrane devises for proton-potassium exchange and a carbonate remover. Hence, the IC system
59 requires a trained operator to ensure top separation capabilities. Yet, once running, an IC instrument
60 is very robust with reproducible performance. IC instruments with both analytical [10] and capillary
61 [11-13] flow modes are available, and both have been used for the analysis of the
62 phosphometabolome. Wang and co-workers compared capIC with both HILIC and RP LC-MS/MS and
63 concluded and superiod resolution and sensitivity of capIC for negatively charged metabolites [13].

64 The metabolomics workflow is elaborate and prone to variation introduced throughout the
65 process of sampling, sample preparation and analysis, and internal standards (IS) are needed to
66 monitor and correlate for the variation introduced [14-16]. Isotope dilution (ID) has been proposed
67 as a strategy to collectively tackle these challenges. A fully uniformly (U) ^{13}C -labeled biological
68 extract is introduced during sample processing stages; thereby, providing a stable isotope analogue
69 for each metabolite. This analogue, which presumably will be degraded at the same rate and ionized
70 at the same efficacy, can be exploited as an IS. Importantly, IS from a ^{13}C extract follow same
71 abundance profiles as the analytes in the real extract which is also preferable compared to IS
72 mixtures with same concentration of all analytes. Many core primary metabolites, e.g. sugar
73 phosphates, are not commercial available in deuterated or ^{13}C labeled form either. Thus, ID enables
74 a reliable quantification of any intracellular metabolite of interest [17].

75 In this short communication, we report on both increased chromatographic separation on a
76 capillary IC (capIC) system and improved quantitative accuracy, precision and robustness combining
77 capIC-MS/MS with ID. The ID strategy is gaining increasing popularity in the quantitative
78 metabolomics field, yet, it poses some challenges related to low abundant metabolites, which are
79 discussed here.

80

81 **2 Materials and Methods**

82

83 **2.1 Standards**

84 79 polar metabolite standards of analytical grade (Supplementary table S1) were purchased from
85 Sigma-Aldrich and Cayman chemicals and prepared as 1 or 10 mM stock solutions in deionized water
86 (DI-water). An external standard mixture (ES) was prepared from stock solutions by serial dilutions,
87 aliquoted and stored at -20°C. Upon analysis, an aliquot of the standard mixture was diluted further
88 to construct a calibration dilution series spanning the concentration range expected for most of the
89 phosphometabolites in biological extracts at the given sampling densities: 5 to 10,000 nM.

90

91 **2.2 Preparation of IS; ¹³C-labeled biomass**

92 *S. cerevisiae* CEN PK was cultivated in a shake flask (0.1 l) at 30°C, 200 rpm, in a mineral medium [18]
93 containing U-¹³C-labeled glucose (> 99%, Cambridge isotope laboratories) as the sole carbon source.
94 At OD₆₆₀ of 1, 10 ml aliquots were withdrawn from the flask and processed as described in 2.4.

95

96 **2.3 Cultivation of microorganisms and human cells for metabolite profiling**

97 The cultivation conditions were optimized to obtain good quality inoculum and for completely usage
98 of the ¹³C-labeled glucose since it is an expensive substrate. *E. coli* was grown in M9 media both in
99 inoculum (shake flasks) and experiment (1L fermenters). *S. cerevisiae* was grown in YNB without
100 amino acids in inoculum (shake flasks) and Verduyn media [18] during experiment (1 L fermentors),
101 both supplemented with 10 g/L glucose. Each experiment started with inoculating shake flasks from
102 cryo vials and grown overnight. 1L media in fermentors were thereafter inoculated to a starting
103 OD₆₆₀ of 0.1 – 0.15 and cultured under controlled conditions until sampling between OD 1 and 2.

104 The human monocytic leukemia cell line THP-1 (ATCC) was cultured in in RPMI-1640 medium
105 (ATCC) supplemented with 50 mL fetal calf serum at 37°C in a humidified atmosphere of 5% CO₂.

106

107

108 **2.4 Sampling and sample preparation**

109 A fast filtration method was applied to separate microbial cells from the media. 10 ml samples were
110 withdrawn from a port in the fermenter, harvested onto 47 mm low protein binding filters
111 compatible with ACN, and fast filtered with controlled vacuum pressure. The vacuum pressure was
112 controlled by CVC 3000 and VSK 3000 units (Vacuubrand GmbH) and optimized for rapid filtration
113 without drying the filters. *S. cerevisiae* was quickly filtered with a pore size of 0.65 µm (Durapore
114 Membrane Filter, PVDF), whereas a two stack filter (Whatman glass fiber filter type GF/C; 1 µm pore
115 size; 47 mm diameter on top of a Pall Supor membrane filter 800; 0.8 µm pore size) was used for *E.*
116 *coli*. The filters were quickly rinsed with 10 ml of cold (0 °C) mineral media followed by a rapid 10-ml
117 cold (0 °C) DI-water rinse lasting less than two seconds, and transferred to a 50 ml centrifuge tube
118 with a 13 ml cold (0°C) solution of 50% Acetonitrile (ACN) in DI-water, which again was transferred
119 to liquid N₂. The adherently growing human cell line was sampled at a cell density of 6*10⁶ cells/dish
120 with quickly removal of the growth medium, washing with cold PBS and DI water, before quenched
121 using a cold ACN-DI water solution. The cells were scraped off and transferred to 50 ML centrifuge
122 tubes and frozen. Metabolite extraction from both human and microbial cells was performed by
123 three freeze-thaw cycles with liquid N₂ and cooling bath kept at 0 °C. The supernatant was aliquoted
124 into four tubes, frozen at -80 °C, further cooled in liquid N₂, lyophilized and stored at -80°C awaiting
125 analysis.

126 Upon analysis, metabolite extracts were dissolved in 500 µL of cold (0°C) DI-water and
127 centrifuged at 14,000rpm, 4 °C for 10 min. The supernatants were carefully transferred onto 3-kD-
128 molecular-weight spin cut-off filters (#516-0228, VWR) and centrifuged at 14,000 rpm, 4 °C for 10
129 minutes.

130

131

132

133 **2.5 CapIC separation**

134 A Thermo Scientific Dionex ICS-4000 capillary IC was operated in external mode with DI-water
135 delivered by an external AXP pump at a flow rate of 30 $\mu\text{l}/\text{min}$. To assist desolvation for better
136 electrospray, a makeup solvent of 90 % ACN in DI-water containing 0.01% ammonium hydroxide
137 (NH_4OH) was delivered by an external AXP-MS pump at 30 $\mu\text{l}/\text{min}$, combined with the eluent via a
138 low dead volume mixing tee and passed through a grounding union before entering the MS. A
139 minimized length of peak tubing (0.08 mm/0.003 in. ID) (#P/N 049715) was used for the capIC-MS
140 interphase. The capIC analysis was performed with a IonPac AS11HC-4 μm , 0.4 \times 250 mm column
141 (2000 Å) and a IonPac AG11-HC 4 μm 0.4x50mm guard column. IC flow rate was 16 $\mu\text{l}/\text{min}$ at 40 °C.
142 The gradient conditions were as follows: an initial 4 mM KOH was held for 1 min, increased to 12
143 mM at 5 min, to 20 mM at 13 min, and 70 mM at 22 min, held at 70 mM for 7.5 min, followed by a
144 rapid increase to 100 mM at 31 min, held 100 mM for 5 min and decreased to 4 mM in 4 min, and
145 finally held for 10 min to re-equilibrate the column. The total run time was 50 min.

146

147 **2.7 MS analysis**

148 A Waters Xevo TQ-S triple-quadrupole MS was operated in negative electrospray ionization (ESI)
149 mode with a capillary voltage of 2.5 kV and ion-source temperature of 150 °C. The desolvation gas
150 was nitrogen, and the flow was set to 800 l/h at a temperature of 300 °C. The collision energy for
151 each MRM transition was optimized for each compound both manually and using the “Intellistart”-
152 function in MassLynx 4.1. The MS was run in dynamic MRM mode, and the retention time (RT)
153 window for each compound was set to ± 2 min of the expected RT. Downstream data processing was
154 performed in MassLynx V4.1.

155

156 **2.8 ID correction**

157 The ¹³C-labelled *S. cerevisiae* extract was added to the ES calibration mixture and the naturally
158 labeled extracts from *S. cerevisiae*, *E. coli* and the human cell line THP-1 at a ratio of 1:5. The ratio of
159 the response area of unlabeled to U¹³C-labeled metabolites was used for correction.

160

161 **3 Results and Discussion**

162 **3.1 Optimization of capIC elution conditions**

163 In principle, optimization of the capIC separation is straightforward as there is only one variable to
164 change; the KOH gradient. Yet, to improve separation of hexose phosphates we also found it
165 necessary to change the column from the recommended Ion Swift MAX 100 column [11, 13] to a
166 AS11-HC column. The latter has higher loading capacity and tolerates higher flow rates. When
167 changing the column and flow rate it was also necessary to optimize the make-up flow, composition
168 of make-up mobile phase, capillary dimensions and back-pressures for stable performance
169 throughout the sequence run [13]. Figure 1A shows the chromatographic separation of an eight
170 hexose phosphate standard mixture on the capIC-MS/MS system with the optimized configuration
171 and elution conditions. Baseline separation was obtained for six out of eight analytes over a seven-
172 minute period, only Mannose 1-phosphate (M1P) and Glucose-1-phosphate (G1P) co-eluted
173 regardless of settings. Importantly, all hexose 6-phosphates were baseline separated, also in
174 biological extracts from three different species; *S. cerevisiae* (Figure 1B), *E. coli* and the human cell
175 line THP-1 (data not shown).

176

177 **3.2 Improved quantitation by ID strategy**

178 IC presents quite stable ionization conditions throughout the gradient run compared to standard LC
179 in both RP and normal phase (NP) where changes in mobile phase composition has a significant
180 effect on ionization. Nevertheless, use of ISs are highly recommended regardless of chromatographic
181 separation technique, as an IS added in the first step of sampling allows for correction of variation
182 introduced throughout the elaborate sample preparation workflow.

183 To evaluate the performance of the ID strategy, an initial test with four injections from
184 parallel samples (individual vials, *S. cerevisiae* extract spiked with ^{13}C *S. cerevisiae* extract) was
185 performed. The relative standard deviation (RSD) decreased from 5 to 1 % when introducing
186 correcting for AMP, and from 4 to 1 % for ATP. As this correction strategy significantly increased
187 quantitative precision for the two tested metabolites, ^{13}C MS/MS transitions were established for all
188 79 metabolites included in the method (Supplementary Table S1: RT, limit of quantitation (LOQ), ^{12}C
189 and ^{13}C MS/MS transitions). By exploiting the U^{13}C -isotope analogue of each metabolite for
190 correction, linearity of most calibration curves was improved (Supplementary Table S2), and the
191 linear range was extended to span all concentrations relevant for the biological extracts.

192

193 **3.3 Challenges related to ID correction**

194 **Low abundant metabolites.** The LOQ, ranging from 1-50 nM for most phosphorylated metabolites
195 and 200-500 nM for most organic acids on the capIC-MS/MS system (Supplementary table S1), is an
196 important parameter to consider for ^{13}C ID correction. For quantitation from biological extracts, the
197 ^{13}C isotope analogue of each metabolite was used for correction when it's concentration was above
198 LOQ. However, when the concentration of a U^{13}C -labeled metabolite is below LOQ in the ^{13}C extract,
199 using this metabolite for correction of the corresponding ^{12}C analogue could lead to erroneous
200 adjustments, as it's concentration is uncertain and varies much more than the concentration of high
201 abundant metabolites. For choosing an alternative ^{13}C IS when the isotope analogue was below LOQ,
202 two criteria was introduced: 1) Similar physico-chemical properties, and 2) similar RT. A metabolite
203 with similar physicochemical properties and RT to the preferred IS metabolite will be degraded at a
204 comparable rate throughout sample preparation, and enter the concentration dependent ion source
205 at approximately the same time, making it the best candidate without severely compromising the
206 properties of the ID correction strategy.

207 The analysis should preferably be run with a complete ES mix, including all metabolites
208 balanced according to their abundance in biological extracts. If the analysis is performed with a

209 reduced ES mix, a third aspect must be considered for selecting candidate IS. The IS mix is a
210 biological extract, with metabolite concentrations varying over several orders of magnitude. Hence,
211 the magnitude of the corrected responses, and the slope of the calibration curves will vary
212 accordingly. Thus, the selected IS and ES must be matched for each metabolite. Ignoring this can
213 cause inaccurate results, deviating in orders of magnitude from the true concentration.

214 **Effect of ID on chromatographic separation.** RT and chromatographic separation was
215 maintained in both ES mixtures and natural labeled biological extracts from *S. cerevisiae*, *E. coli* and
216 human THP-1 cells when added ¹³C *S. cerevisiae* extract for close to all metabolites, the exception
217 being hexose phosphates. Surprisingly, several of the hexose phosphates that were baseline
218 separated in natural labeled ES mixtures and biological extracts (lower panel Figure 2A and B,
219 respectively) co-eluted when spiked with ¹³C *S. cerevisiae* extract (Figure 2, upper panel). Figure 2A
220 depicts how Fructose 6-phosphate (F6P) (RT 11.5) has merged with the G6P (RT 11.1), with a slight
221 shift in RT. The hexose 1-phosphates are seemingly unaffected. The effect was consistent across
222 pure ES and biological extracts from the three tested species, and could not be counteracted by
223 altering chromatographic conditions nor sample preparation. Spiking with a ¹³C *S. cerevisiae* extract
224 does not exceed the column loading capacity as the natural labeled extract is reduced
225 proportionately. Hence, if individual quantitation of hexose-6-phosphates is required, samples must
226 be re-run without ¹³C *S. cerevisiae* extract. ID has recently been introduced in non-target
227 Metabolomics [10], and these results demonstrates that great care must be taken with this strategy,
228 as mixing extracts can introduce bias and artefacts which is harder to identify in a non-target
229 approach.

230

231 **3.4 Assessment of long term stability**

232 Metabolite profiling with capIC-MS/MS is not high throughput; a sample run is 30-60 minutes long
233 depending on the metabolites included in the method and the required level of separation.

234 Comprehensive studies can result in sample lists with over 100 injections including biological and

235 technical replicates from each sampled condition, blanks, ES calibration series and quality controls
236 (QCs), implying that the analysis will last for days/week(s). Thus, maintained precision of the system
237 is critical, and the final step in this method upgrade project was to monitor and evaluate the system
238 performance over a 10-day period with >200 injections. Individual samples are not presented, as
239 they cannot be used to evaluate technical precision solely, but an average RSD of 23% between
240 biological replicas was measured for the human cell line THP-1, this including biological variation
241 between separate culture dishes and variation introduced during sample preparation and capIC-ID-
242 MS/MS analysis. Table 1 lists the RSD between 10 injections, each separated in time by one day, for
243 a 5 μ M ATP standard sample and ATP, ADP and AMP in five THP-1 QC cell extracts. The RSD between
244 samples was drastically reduced, especially for ATP and AMP. Clearly, 13 C ID correction improves the
245 quantitative precision.

246 In conclusion, the presented capIC-MS/MS method including ID correction and covering
247 almost 80 metabolites provides high chromatographic separation capabilities and a reliable
248 quantitative profiling of the phosphometabolome. Figure 3 visualizes the comprehensive coverage of
249 primary metabolite pools by the capIC-MS/MS and the heat mapping indicates the large variation in
250 concentration among the primary metabolites.

251

252 **Acknowledgements**

253 This project was supported by the Norwegian Research Council (grant number 237165) as part of the
254 Era-IB project Terpenosome (MHS) and by NTNU Enabling Biotechnology PhD grant (LMR).

255

256 **References**

- 257 [1] A. Gil, D. Siegel, H. Permentier, D.J. Reijngoud, F. Dekker, R. Bischoff, Stability of energy
258 metabolites An often overlooked issue in metabolomics studies: A review, *Electrophoresis*, 36 (2015)
259 2156-2169.
260 [2] D. Siegel, H. Permentier, D.J. Reijngoud, R. Bischoff, Chemical and technical challenges in the
261 analysis of central carbon metabolites by liquid-chromatography mass spectrometry, *Journal of*
262 *chromatography. B, Analytical technologies in the biomedical and life sciences*, 966 (2014) 21-33.

263 [3] I. Aretz, D. Meierhofer, Advantages and Pitfalls of Mass Spectrometry Based Metabolome
264 Profiling in Systems Biology, *International journal of molecular sciences*, 17 (2016).

265 [4] H.F.N. Kvitvang, T. Andreassen, T. Adam, S.G. Villas-Boas, P. Bruheim, Highly Sensitive GC/MS/MS
266 Method for Quantitation of Amino and Nonamino Organic Acids, *Analytical Chemistry*, 83 (2011)
267 2705-2711.

268 [5] O.I. Savolainen, A.-S. Sandberg, A.B. Ross, A Simultaneous Metabolic Profiling and Quantitative
269 Multimetabolite Metabolomic Method for Human Plasma Using Gas-Chromatography Tandem Mass
270 Spectrometry, *Journal of Proteome Research*, 15 (2016) 259-265.

271 [6] Y. Shen, T. Fatemeh, L. Tang, Z. Cai, Quantitative metabolic network profiling of *Escherichia coli*:
272 An overview of analytical methods for measurement of intracellular metabolites, *TrAC Trends in*
273 *Analytical Chemistry*, 75 (2016) 141-150.

274 [7] P. Bruheim, H.F.N. Kvitvang, S.G. Villas-Boas, Stable isotope coded derivatizing reagents as
275 internal standards in metabolite profiling, *Journal of Chromatography A*, 1296 (2013) 196-203.

276 [8] B. Luo, K. Groenke, R. Takors, C. Wandrey, M. Oldiges, Simultaneous determination of multiple
277 intracellular metabolites in glycolysis, pentose phosphate pathway and tricarboxylic acid cycle by
278 liquid chromatography-mass spectrometry, *Journal of Chromatography A*, 1147 (2007) 153-164.

279 [9] R.M. Seifar, C. Ras, J.C. van Dam, W.M. van Gulik, J.J. Heijnen, W.A. van Winden, Simultaneous
280 quantification of free nucleotides in complex biological samples using ion pair reversed phase liquid
281 chromatography isotope dilution tandem mass spectrometry, *Analytical biochemistry*, 388 (2009)
282 213-219.

283 [10] M. Schwaiger, E. Rampler, G. Hermann, W. Miklos, W. Berger, G. Koellensperger, Anion-
284 Exchange Chromatography Coupled to High-Resolution Mass Spectrometry: A Powerful Tool for
285 Merging Targeted and Non targeted Metabolomics, *Analytical Chemistry*, 89 (2017) 7667-7674.

286 [11] H.F.N. Kvitvang, K.A. Kristiansen, P. Bruheim, Assessment of capillary anion exchange ion
287 chromatography tandem mass spectrometry for the quantitative profiling of the
288 phosphometabolome and organic acids in biological extracts, *Journal of Chromatography A*, 1370
289 (2014) 70-79.

290 [12] K. Burgess, D. Creek, P. Dewsbury, K. Cook, M.P. Barrett, Semi-targeted analysis of metabolites
291 using capillary-flow ion chromatography coupled to high-resolution mass spectrometry, *Rapid*
292 *Commun. Mass Spectrom.*, 25 (2011) 3447-3452.

293 [13] J. Wang, T.T. Christison, K. Misuno, L. Lopez, A.F. Huhmer, Y. Huang, S. Hu, Metabolomic
294 Profiling of Anionic Metabolites in Head and Neck Cancer Cells by Capillary Ion Chromatography with
295 Orbitrap Mass Spectrometry, *Analytical Chemistry*, 86 (2014) 5116-5124.

296 [14] H.F.N. Kvitvang, P. Bruheim, Fast filtration sampling protocol for mammalian suspension cells
297 tailored for phosphometabolome profiling by capillary ion chromatography - tandem mass
298 spectrometry, *Journal of Chromatography B-Analytical Technologies in the Biomedical and Life*
299 *Sciences*, 998 (2015) 45-49.

300 [15] S.G. Villas-Boas, P. Bruheim, Cold glycerol-saline: The promising quenching solution for accurate
301 intracellular metabolite analysis of microbial cells, *Analytical biochemistry*, 370 (2007) 87-97.

302 [16] T.J. Causon, S. Hann, Review of sample preparation strategies for MS-based metabolomic
303 studies in industrial biotechnology, *Analytica Chimica Acta*, 938 (2016) 18-32.

304 [17] L. Wu, M.R. Mashego, J.C. van Dam, A.M. Proell, J.L. Vinke, C. Ras, W.A. van Winden, W.M. van
305 Gulik, J.J. Heijnen, Quantitative analysis of the microbial metabolome by isotope dilution mass
306 spectrometry using uniformly ¹³C-labeled cell extracts as internal standards, *Analytical*
307 *biochemistry*, 336 (2005) 164-171.

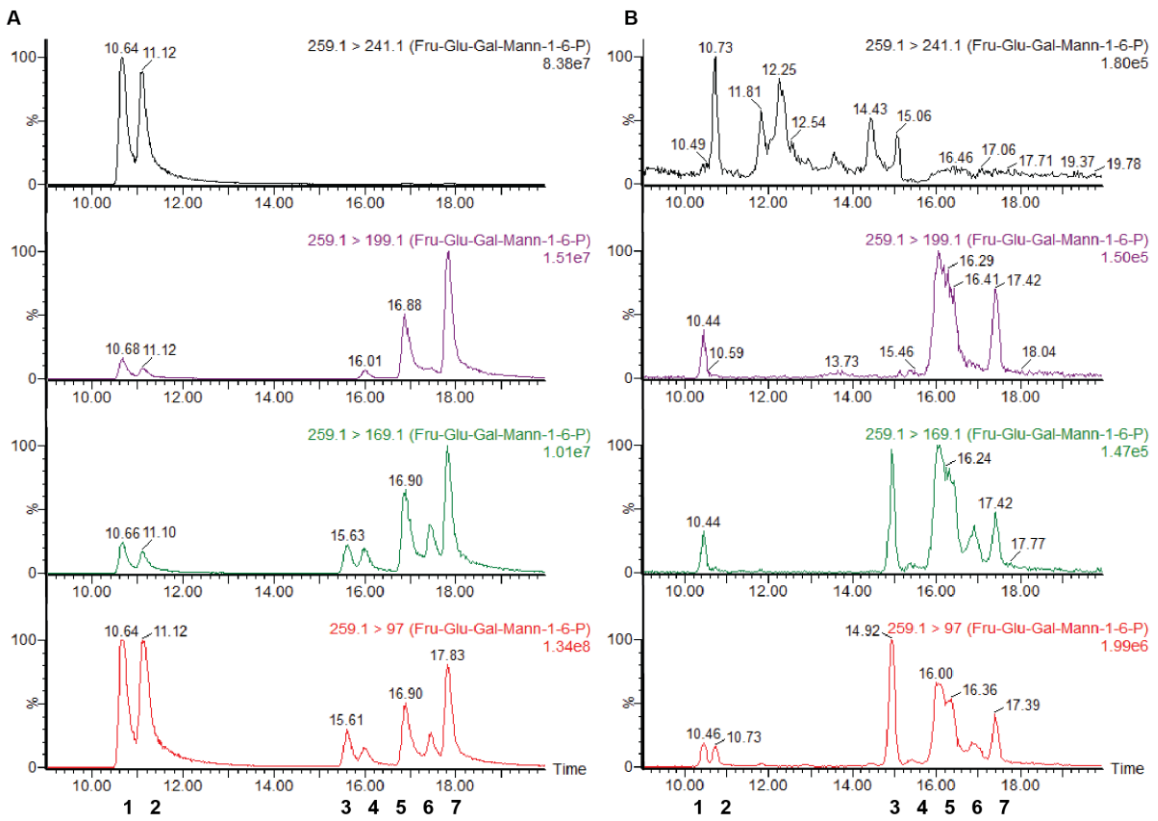
308 [18] C. Verduyn, A.H. Stouthamer, W.A. Scheffers, J.P. Vandijken, A Theoretical evaluation of growth
309 yields of yeasts, *Antonie Van Leeuwenhoek International Journal of General and Molecular*
310 *Microbiology*, 59 (1991) 49-63.

311

312

Figure legends

Figure 1



313

314 Figure 1. Extracted ion chromatogram for hexose phosphate MS/MS transitions for an ES mixture (A)

315 and a *S.cerevisiae* extract (B). The hexose phosphates included are 1: GAL1P; 2: M1P+G1P; 3: F1P; 4:

316 GAL6P; 5: G6P; 6:F6P; 7: M6P (Abbreviations listed in Supplementary Table S3).

317

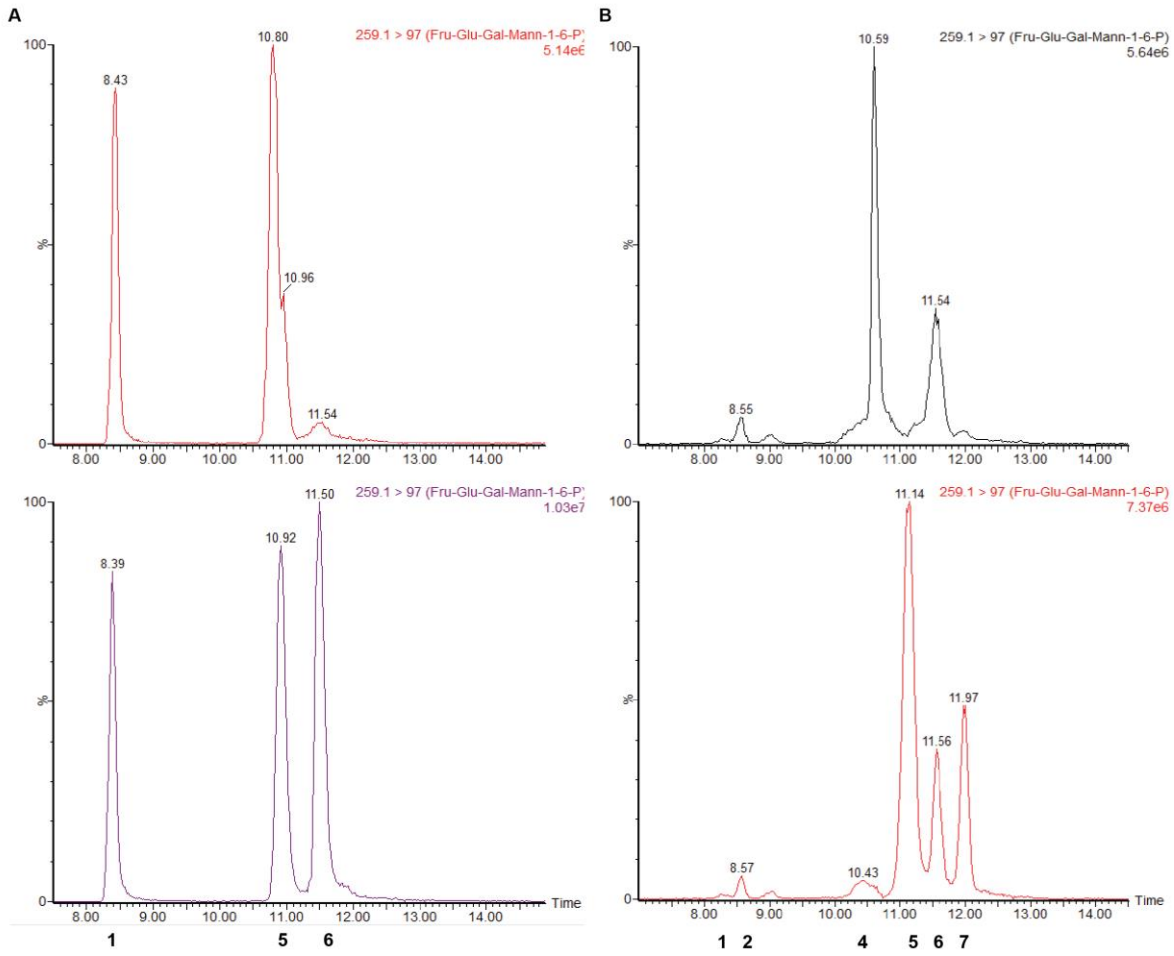
318

319

320

321

Figure 2



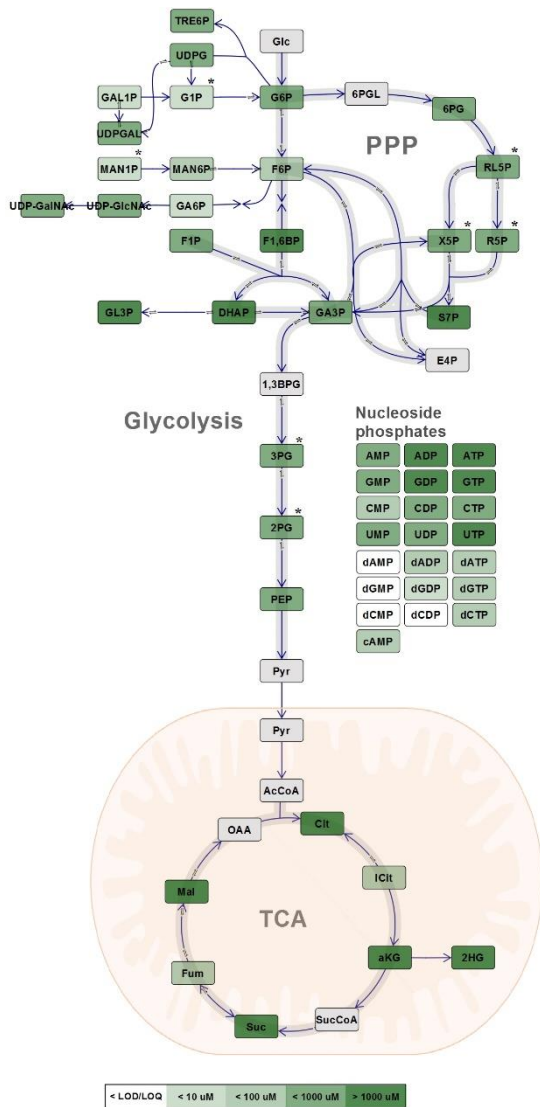
322

323

324 Figure 2. Extracted ion chromatogram for hexose phosphates (m/z 259.1 \rightarrow 97 transition) of a
325 three-hexose phosphate mixture (A) and an *E. coli* DH5 α extract (B) with (upper panel) and without
326 (lower panel) ¹³C *S. cerevisiae* extract added. The hexose phosphates included are 1: GAL1P; 2:
327 M1P+G1P; 3: F1P; 4: GAL6P; 5: G6P; 6:F6P; 7: M6P (Abbreviations listed in Supplementary Table 3).

328

329



330

331 Figure 3. Visualization of the comprehensive coverage of primary metabolite pools by the present
 332 capIC method. Data is taken from a *Saccharomyces cerevisiae* batch cultivation in mineral medium
 333 and the heat mapping shows how the metabolite pools are varying over 4 orders of magnitude.

334 Table 1. Instrument performance over a 10-day period for three selected metabolites (ATP, ADP and
 335 AMP). Each sample (a 5 μ M ES mixture and 5 identical biological samples; (QCs) was injected once per
 336 day over a 10-day period. The table lists RSD between the ten injections for non-correlated results
 337 (Area) and results correlated with 13 C IS (Response factor).

	ATP		ADP		AMP	
	Area	Response factor	Area	Response factor	Area	Response factor
ES mix (5 μ M)	39	13	22	24	14	15
QC1	23	14	19	23	41	11
QC2	25	6	48	18	15	5
QC3	47	4	23	11	41	3
QC4	26	3	35	25	26	3
QC5	30	3	17	14	49	11

338

339

340

341 **Supplementary Table S1**

342 Complete MS/MS settings for metabolites included in the method. LOQ is determined according to
 343 Kvitvang et al [11].. Abbreviations are listed in Supplementary Table S3.

Metabolite	RT (min)	Collision energy (V)	¹² C		U ¹³ C-IS		LOQ (nM)
			[M-H] (Q1)	Q3	[M-H] (Q1)	Q3	
PYR	5.0		87.0		90.0		
LAC	3.4		89.0		90.0		
FUM	15.4	8	115.1	71.1	119.0	75.0	200
ACTP	20.8	15	139.0	79.0	141.0	79.0	50
SUC	11.9	10	117.1	73.1	121.0	76.0	500
IA	13.5	10	129.1	85.0	131.0	85.0	25
MAL	11.9	14	133.1	71.1	137.0	74.0	300
aKG*	11.7	8	145.0	101.0	150.0	106.0	300
2-HG	11.6	16	147.1	85.1	152.0	89.0	300
PEP	22.1	12	167.0	79.0	170.0	79.0	5
DHAP	24.1	8	169.0	97.0	172.0	79.0	1
G3P	22.9	14	169.0	79.0	172.0	79.0	1
GL3P	10.6	14	171.0	79.0	174.0	79.0	50
2-IPPMAL	14,1	14	175.1	85.0	182.1	120.0	500
2PG+3PG	21.4	12	185.0	97.0	188.0	97.0	400
ICIT	22.4	18	191.0	73.1	197.0	116.0	25
CIT	21.2	16	191.1	87.1	197.0	116.0	75
DOXP	11.2	23	213.0	139.0	218.0	79.0	1
MEP	10.6	13	215.0	79.0	220.0	79.0	1
RL5P+R5P+X5P	16.2	10	229.1	96.8	234.0	97.0	5
DMAPP	23.2	14	245.0	79.0	250.0	79.0	1
IPP	23.4	14	245.0	79.0	250.0	79.0	1
GA1P	9.3	16	258.0	97.0	264.0	97.0	0,5
GA6P	15.3	16	258.0	97.0	264.0	97.0	2
F1P	14.8	12	259.1	97.0	265.0	97.0	1
F6P	16.7	14	259.1	97.0	265.0	97.0	20
G1P	10.6	20	259.1	241.0	265.0	247.0	10
M1P	10.6	20	259.1	241.0	265.0	247.0	1
G6P	16.3	14	259.1	97.0	265.0	97.0	20
GAL1P	10.0	14	259.1	97.0	265.0	97.0	20
GAL6P	15.5	14	259.1	97.0	265.0	97.0	1
M6P	17.4	16	259.1	97.0	265.0	97.0	5
1-IP1	10.0	14	259.1	97.0			1
3-IP1	10.0	14	259,1	97.0			1
4-IP1	10.6	14	259,1	97.0			1
6PG	20.5	16	275.1	97.0	281.1	97.0	20
S7P	17.8	20	289.0	97.0	296.0	97.0	10
dUMP	21.3	16	307.1	195.0	316.0	200.0	1

GPP	36.0	18	313.1	79.0	318.1	79.0	0,5
dTMP	21.9	16	321.1	195.0	331.1	200.0	25
CMP	12.7	20	322.0	79.0	331.0	79.0	10
UMP	23.0	20	323.2	97.0	332.1	97.0	25
cAMP	13.8	26	328.1	134.2	338.1	139.1	10
dAMP	14.7	14	330.1	195.0	340.0	200.0	25
F1,6BP	25.0	20	339.1	97.0	345.1	97.0	50
4,5-IP2	24.5	15	339.1	241.0	345.1	97.0	1
1,4,5-IP3	30.8	15	339.1	241.0	419.1	339.1	0,5
cGMP	24.5	22	344.1	150.0	354.0	152.0	10
AMP	17.8	30	346.1	79.0	356.1	79.0	5
IMP	25.2	22	347.2	79.0	357.0	79.0	50
GMP	25.4	24	362.1	79.0	372.0	79.0	1
FPP	36.6	16	381.1	79.0			1
PRPP	27.4	14	388.9	177.1	394.0	177.1	1
dTDP	26.0	22	401.1	159.0	411.1	158.9	100
CDP	21.7	26	402.1	159.0	411.1	158.9	5
UDP	27.0	20	403.1	110.9	412.1	115.1	10
dADP	22.7	24	410.1	159.0	420.1	158.9	25
T6P	10.4	23	422.0	241.0	434.0	242.0	1
ADP	23.9	26	426.1	159.0	436.1	139.1	25
dGDP	27.5	38	426.1	275.1	436.1	280.1	10
GDP	32.0	18	442.1	344.2	452.1	155.1	100
GGPP	24.5	25	449.0	79.0			5
dCTP	23.9	34	466.1	159.0	175.1	158.9	1
dUTP	30.4	24	467.1	159.0	476.1	158.9	10
dTTP	31.6	34	481.1	159.0	491.1	159.0	25
CTP	25.1	34	482.1	159.0	491.1	158.9	25
UTP	33.7	34	483.1	159.0	492.1	158.9	25
dATP	26.1	30	490.1	159.0	500.1	158.9	2
ATP	27.6	32	506.1	159.0	516.1	158.9	50
dGTP	34.1	32	506.1	159.0	516.1	158.9	1
ITP	34.6	36	507.1	159.0	517.1	158.9	10
GTP	35.9	30	522.1	159.0	532.1	158.9	10
UDPG+UDPGAL	(22+)22,4	22	565.0	323.0	580.0	323.0	1
UDP-GlcNAc+UDP-GalNAc	21.4	26	606.2	385.1	623.6	394.1	10

344

345

346 **Supplementary Table S2**347 Coefficients of determination (R^2) obtained from non-correlated and correlated ^{13}C IS calibration
348 lines.

Metabolite	R^2 calibration curve	
	Without ^{13}C IS	With ^{13}C IS
ADP	0.988	0.996
AMP	0.997	0.998
ATP	0.998	0.998
CIT	0.992	0.912
CMP	0.996	0.999
dADP	0.968	0.999
dAMP	0.999	0.989
dATP	0.973	0.999
DOXP	0.999	0.999
F1P	0.988	0.999
FUM	0.996	0.998
GAL1P	0.993	0.999
GTP	0.997	0.999
IA	0.973	0.997
ICIT	0.972	0.854
M6P	0.998	0.999
RL5P+R5P+X5P	0.999	0.998
S7P	0.996	0.999
TTP	0.997	0.997
UDP-Glc/Gal-Nac	0.988	0.999

349

350

351 **Supplementary Table 3. List of abbreviations**

352

353	1,4,5-IP ₃	Inositol-1,4,5-triphosphate
354	1-IP ₁	Inositol 1-phosphate
355	2-HG	2-Hydroxyglutarate
356	2-IPPMAL	2-Isopropylmalate
357	2PG+3PG	2-Phosphoglycerate, 3-Phosphoglycerate
358	3-IP ₁	Inositol 3-phosphate
359	4,5-IP ₂	Inositol 4,5-diphosphate
360	4-IP ₁	Inositol 4-phosphate
361	6PG	6-phosphogluconate
362	ACTP	Acetyl-phosphate
363	ADP	Adenosine diphosphate
364	aKG	α-Ketoglutarate
365	AMP	Adenosine monophosphate
366	ATP	Adenosine triphosphate
367	cAMP	cyclic adenosine monophosphate
368	cGMP	cyclic guanosine monophosphate
369	CIT	Citrate
370	CDP	Cytidine diphosphate
371	CMP	Cytidine monophosphate
372	CTP	Cytidine triphosphate
373	DHAP	Dihydroxyacetone phosphate
374	DMAPP	Dimethylallyl pyrophosphate
375	DOXP	1-deoxy-D-xylulose 5-phosphate
376	dADP	Deoxy-adenosine diphosphate
377	dAMP	Deoxy-adenosine monophosphate
378	dATP	Deoxy-adenosine triphosphate
379	dCTP	Deoxy-cytidine triphosphate
380	dGDP	Deoxy-guanosine diphosphate
381	dGTP	Deoxy-guanosine triphosphate
382	dTDP	Deoxy-thymidine diphosphate

383	dTMP	Deoxy-thymidine monophosphate
384	dTTP	Deoxy-thymidine triphosphate
385	dUMP	Deoxy-uridine monophosphate
386	dUTP	Deoxy-uridine diphosphate
387	F1,6BP	Fructose 1,6-bisphosphate
388	F1P	Fructose 1-phosphate
389	F6P	Fructose 6-phosphate
390	FPP	Farnesyl pyrophosphate
391	FUM	Fumarate
392	G1P	Glucose 1-phosphate
393	G6P	Glucose 6-phosphate
394	GA1P	Glucoseamine 1-phosphate
395	G3P	Glyceraldehyde 3-phosphate
396	GA6P	Glucoseamine 6-phosphate
397	GAL1P	Galactose 1-phosphate
398	GAL6P	Galactose 6-phosphate
399	GDP	Guanosine diphosphate
400	GGPP	Geranylgeranyl pyrophosphate
401	GL3P	Glycerol 3-phosphate
402	GMP	Guanosine monophosphate
403	GPP	Geranyl pyrophosphate
404	GTP	Guanosine triphosphate
405	IA	Itaconic acid
406	ICIT	Isocitrate
407	IMP	Inosine monophosphate
408	IPP	Isopentenyl pyrophosphate
409	ITP	Inosine triphosphate
410	LAC	Lactate
411	M1P	Mannose 1-phosphate
412	M6P	Mannose 6-phosphate
413	MAL	Malate
414	MEP	2-C-methyl-D-erythritol 4-phosphate

415	PEP	Phosphoenolpyruvate
416	PRPP	Phosphoribosyl pyrophosphate
417	PYR	Pyruvate
418	RL5P+R5P+X5P	Ribulose 5-phosphate, Ribose 5-phosphate, Xylulose 5-phosphate
419	S7P	Sedoheptulose 7-phosphate
420	SUC	Succinate
421	T6P	Trehalose-6-phosphate
422	UDP	Uridine diphosphate
423	UDPG+UDPGAL	UDP Glucose, UDP Galactose
424	UDP-GlcNAc+UDP-GalNAc	UDP N-acetylglucosamine, UDP N-acetylgalactosamine
425	UMP	Uridine monophosphate
426	UTP	Uridine triphosphate